http://dx.doi.org/10.62762/TSCC.2025.553018

RESEARCH ARTICLE

A Safety-Critical Control Scheme for Spacecraft Relative Motion Tracking Based on the Fully Actuated System Approach and Offline QP Solutions

Xiaoyu Yang[1,2,3], **Qiang Chen**[1,2,3,*] **and Xiongxiong He**[1,2,3]

[1] College of Information Engineering, Zhejiang University of Technology, Hangzhou 310014, China
[2] Zhejiang Key Laboratory of Intelligent Perception and Control for Complex Systems, Zhejiang University of Technology, Hangzhou 310014, China
[3] State Key Laboratory of Green Chemical Synthesis and Conversion, Zhejiang University of Technology, Hangzhou 310014, China

Abstract

A safety-critical control scheme based on fully actuated system approach (FASA) framework is developed for spacecraft relative motion tracking under external disturbances and multiple forbidden regions. For tracking performance, the nominal controller is designed by using the FASA framework, such that the controller design process can be simplified. For safety constraints, a disturbance-tolerant control barrier function incorporating low-pass filtered disturbance compensation is introduced to mitigate interference effects. Furthermore, a sequential correction strategy is developed to resolve safety constraints through offline-computed quadratic program (QP) solutions, which can eliminate dependence on real-time optimization of the QP solver. Theoretical analysis confirms that the proposed control scheme simultaneously guarantees collision avoidance and the spacecraft relative motion tracking. Numerical simulations further validate the effectiveness of the proposed approach.

Keywords: control barrier function, fully actuated system approach, safety-critical control, spacecraft relative motion tracking.

1 Introduction

In recent years, with the rapid development of space missions such as on-orbit servicing, space station maintenance, and constellation coordination [1–3], precise tracking and control technology for close-range relative motion between spacecraft has emerged as a research frontier in aerospace engineering. The primary control objective for such missions lies in enabling the follower spacecraft to achieve highly reliable relative position tracking with respect to the leader spacecraft or a desired orbit. To achieve this control goal, several control approaches, including PID control [4–6], sliding mode control (SMC) [7–9] and backstepping control (BSC) [10–12], have been theoretically proposed.

While nonlinear control techniques including PID

Submitted: 31 October 2025
Accepted: 12 January 2026
Published: 17 March 2026

Vol. 3, **No.** 1, 2026.
10.62762/TSCC.2025.553018

***Corresponding author:**
✉ Qiang Chen
sdnjchq@zjut.edu.cn

Citation
Yang, X., Chen, Q., & He, X. (2026). A Safety-Critical Control Scheme for Spacecraft Relative Motion Tracking Based on the Fully Actuated System Approach and Offline QP Solutions. *ICCK Transactions on Sensing, Communication, and Control*, 3(1), 54–63.

control, SMC, and BSC offer certain benefits, the resulting closed-loop systems generally maintain nonlinear characteristics. Recently, fully-actuated system approach (FASA) [13–16] has gained increasing attention due to its demonstrated effectiveness and simplicity in addressing nonlinearities in dynamical systems. A distinctive advantage of FASA is its ability to produce a linear time-invariant closed-loop system through appropriate controller design. However, in practical missions, spacecraft must operate in highly constrained environments populated by substantial space debris. The traditional FASAs [13–16] generally lack active safety constraints on system state trajectories, failing to guarantee continuous obstacle avoidance throughout the entire control process. Consequently, safety must be explicitly considered in the design of spacecraft relative motion tracking control.

To address the aforementioned safety challenges, control barrier functions (CBFs) have been explored for dynamical systems [17–19]. The core advantage of CBFs lies in their ability to embed safety requirements into controller design through mathematical constraints, thereby providing provable safety guarantees for systems. Typically, CBFs are computationally efficient and can be readily integrated with performance-oriented controllers. For example, A safety-critical methodology integrates CBFs with control Lyapunov functions through quadratic programming (QP), aiming to balance safety with performance objectives for control-affine systems [20]. Several CBF-QP variants have been proposed, such as high-order CBFs to address high-order nonlinear systems [21] and robust CBFs that account for worst-case disturbances [22]. Recent efforts have also focused on mitigating the conservatism of robust approaches. For instance, disturbance rejection CBFs leverage disturbance observers to handle mismatched disturbances more effectively [23]. Despite these advancements, a fundamental limitation persists across most existing CBF-QP methods [17–23]: their reliance on real-time QP solutions. This dependency introduces significant practical challenges for spacecraft applications: (i) Computational delays: As environmental complexity increases with multiple forbidden regions, the dimensionality of the QP problem grows, potentially causing solvers to exceed control periods and endangering real-time obstacle avoidance. (ii) Resource burden: The computational load of continuous QP solving competes with other critical spacecraft functions like navigation and communication, while effective disturbance rejection necessitates short control periods, further straining computational resources. Based on the comprehensive review of the literature, few studies have addressed safety-critical control problems with multiple safety constraints via offline QP synthesis.

This paper develops a safety-critical control scheme based on FASA framework for spacecraft relative motion tracking under external disturbances and multiple forbidden regions. The main contributions of the paper are summarized as follows:

1) A safety-critical control framework integrating the FASA with CBF-based safety design is developed for spacecraft relative motion tracking, such that the tracking performance and safety constraints can be simultaneously achieved.

2) In contrast to conventional CBF-QP methods that rely on real-time optimization [17–23], this paper develops a safety-critical control scheme based on a sequential correction mechanism, where a series of QPs incorporating disturbance-tolerant CBF (DTCBF) constraints are solved offline to eliminate the computational delay and burden of real-time QP solvers.

The paper is structured as follows. Section 2 formulates the problem formulation and preliminaries. Section 3 presents the FASA-based safety-critical control protocol for spacecraft relative motion tracking. The simulations are detailed in Section 4. Finally, conclusion is summarized in Section 5.

2 Problem Formulation and Preliminaries

As illustrated in Figure 1, the relative motion of the spacecraft is defined with respect to two coordinate systems: the Earth-centered inertial (ECI) frame $(O_E - XYZ)$ and the local-vertical-local-horizontal (LVLH) frame $(o - xyz)$. In the presence of external disturbances—such as those arising from Earth's non-spherical gravitational perturbations and atmospheric drag—conventional safety-critical control strategies may fail to prevent collisions, while typical robust safety-critical controllers tend to produce overly conservative trajectories.

The relative motion dynamics of the follower spacecraft in LVLH frame can be expressed as

$$M\ddot{\boldsymbol{p}} = \boldsymbol{C}(\dot{\theta})\dot{\boldsymbol{p}} + \big(\boldsymbol{J}(\dot{\theta},\ddot{\theta}) - \frac{\mu M}{R^3}\boldsymbol{I}_3\big)\boldsymbol{p} + \boldsymbol{h} + \boldsymbol{u} + \boldsymbol{d}, \tag{1}$$

where $\boldsymbol{C}(\dot{\theta}) = 2M[0,\dot{\theta},0;-\dot{\theta},0,0;0,0,0]^T \in \mathbb{R}^{3\times3}$, $\boldsymbol{C}(\dot{\theta}) = M[\dot{\theta}^2,\ddot{\theta},0;-\ddot{\theta},\dot{\theta}^2,0;0,0,0]^T \in \mathbb{R}^{3\times3}$, $\dot{\theta} = n_c(1+e_c\cos(\theta))^2/(1+e_c^2)^{3/2}$ is the evolution of the true anomaly θ, $n_c = (\mu/a_c^3)^{1/2}$, a_c, and e_c are mean orbital angular velocity, semimajor axis and eccentricity of leader spacecraft, respectively. $\boldsymbol{p} = [p_1,p_2,p_3]^T \in \mathbb{R}^3$ is the spacecraft relative position vector. $\boldsymbol{u} = [u_1,u_2,u_3]^T \in \mathbb{R}^3$ and $\boldsymbol{d} = [d_1,d_2,d_3]^T \in \mathbb{R}^3$ are the input force and external disturbances, respectively. $\boldsymbol{h} = \mu M[-R_c/R^3 + 1/R_c^2,0,0]^T \in \mathbb{R}^3$, $R = \sqrt{(R_c+p_1)^2+p_2^2+p_3^2}$. μ and R_c are gravitational constant and the distance between the leader spacecraft and center of Earth. M is the mass of follower spacecraft.

By defining $\boldsymbol{x} = [\boldsymbol{p}^T,\dot{\boldsymbol{p}}^T]^T$, the dynamic system (1) is given as

$$\dot{\boldsymbol{x}} = \boldsymbol{f} + \boldsymbol{g}(\boldsymbol{u}+\boldsymbol{d}+\boldsymbol{\zeta}), \tag{2}$$

where $\boldsymbol{f} = \bar{\boldsymbol{A}}\boldsymbol{x}$, $\bar{\boldsymbol{A}} = \begin{bmatrix}\boldsymbol{0}_{3\times3} & \boldsymbol{I}_3\\ \boldsymbol{0}_{3\times3} & \boldsymbol{0}_{3\times3}\end{bmatrix} \in \mathbb{R}^{6\times6}$, $\boldsymbol{g} = [\boldsymbol{0}_{3\times3}, 1/M\boldsymbol{I}_3]^T \in \mathbb{R}^{6\times3}$, and $\boldsymbol{\zeta} = \boldsymbol{C}(\dot{\theta})\dot{\boldsymbol{p}} + (\boldsymbol{J}(\dot{\theta},\ddot{\theta}) - (\mu M/R^3)\boldsymbol{I}_3)\boldsymbol{p} + \boldsymbol{h}$.

To achieve relative motion tracking of spacecraft systems, following assumption and lemmas are listed blow:

Assumption 1 [24] *The disturbance $\boldsymbol{d}$ and its derivative $\dot{\boldsymbol{d}}$ are bounded, i.e., $\|\boldsymbol{d}\| \le \breve{D}$ and $\|\dot{\boldsymbol{d}}\| \le \breve{d}$ hold for $\breve{D} \ge 0$ and $\breve{d} \ge 0$.*

Lemma 1 [25] *Consider a matrix $\boldsymbol{\Phi} \in \mathbb{R}^{6\times6}$ that satisfies $Re\lambda_j(\boldsymbol{\Phi}) \le -\frac{\delta}{2}$, where $j \in [1,\dots,6]$, $\lambda_j(\boldsymbol{\Phi})$ is the jth eigenvalue of the matrix $\boldsymbol{\Phi}$, and δ is a positive constant. Then, the following inequality holds*

$$\boldsymbol{Q}^T\boldsymbol{\Phi} + \boldsymbol{\Phi}\boldsymbol{Q} \le -\delta\boldsymbol{Q}, \tag{3}$$

where $\boldsymbol{Q}$ is a positive-definite matrix.

Lemma 2 [26] *Consider a differential inequality given as $\dot{b} \ge -\xi(b)$ with $b(0) \ge 0$ for $t \in [0,+\infty)$, where $h \in \mathbb{R}$ is a continuously differentiable function, and $\xi(b)$ is a class $\mathcal{K}$ function. Then $b \ge 0$ for $t \in [0,+\infty)$.*

3 Main Results

This section presents the low-pass filters to design disturbance compensation term. The control input is structured as $\boldsymbol{u} = \boldsymbol{u}_0 + \sum_{i=1}^{N}\boldsymbol{u}_{si}$, and the set of unsafe regions is denoted by $\mathcal{O}\{O_1,\dots,O_N\}$, where N represents the total number of such regions encountered along the orbit. $\boldsymbol{u}_0$ acts as the FASA nominal controller, designed to achieve trajectory tracking, while each $\boldsymbol{u}_{si}, (i = 1,\dots,N)$ serves as a safety correction term, steering the spacecraft away from the ith unsafe region.

3.1 Disturbance Compensation Design

Define $\boldsymbol{x}_2 = \dot{\boldsymbol{p}}$, the subsystem of (2) can be rewritten as

$$\dot{\boldsymbol{x}}_2 = \frac{1}{M}(\boldsymbol{d}+\bar{\boldsymbol{\zeta}}), \tag{4}$$

where $\bar{\boldsymbol{\zeta}} = \boldsymbol{u} + \boldsymbol{\zeta}$.

The low-pass filter transformation is applied to system (4), one yields

$$\dot{\boldsymbol{x}}_{2f} = \frac{1}{M}(\hat{\boldsymbol{d}} + \bar{\boldsymbol{F}}_f), \tag{5}$$

where $\boldsymbol{x}_{2f}$, $\hat{\boldsymbol{d}}$, and $\bar{\boldsymbol{F}}_f$ are filtered variables of $\boldsymbol{x}_2$, $\boldsymbol{d}$, $\bar{\boldsymbol{F}}$.

Inspired by [27] the following low-pass filter transformation is designed to estimate the disturbance

$$\begin{cases}\gamma\dot{\boldsymbol{x}}_{2f} + \boldsymbol{x}_{2f} = \boldsymbol{x}_2,\\ \gamma\dot{\bar{\boldsymbol{\zeta}}}_f + \bar{\boldsymbol{\zeta}}_f = \bar{\boldsymbol{\zeta}}.\end{cases} \tag{6}$$

For the spacecraft system (1), the estimation of $\boldsymbol{d}$ is constructed as follows

$$\hat{\boldsymbol{d}} = \frac{M}{\gamma}(\boldsymbol{x}_2 - \boldsymbol{x}_{2f}) - \bar{\boldsymbol{\zeta}}_f. \tag{7}$$

Theorem 1 *For the spacecraft system (1) subject to disturbance $\boldsymbol{d}$, the disturbance compensation term (7) ensures that the estimation error $\tilde{\boldsymbol{d}} = \boldsymbol{d} - \hat{\boldsymbol{d}}$ converges to a bounded region*

$$\Omega_{\tilde{d}} = \left\{\tilde{\boldsymbol{d}} \mid \|\tilde{\boldsymbol{d}}\| \le \left(2\exp(-\frac{t}{\gamma})\|\tilde{\boldsymbol{d}}(0)\|^2 + \gamma^2\breve{d}^2\right)^{\frac{1}{2}}\right\}. \tag{8}$$

Proof 1 *Define a Lyapunov function as*

$$V_0 = \frac{1}{2}\tilde{\boldsymbol{d}}^T\tilde{\boldsymbol{d}}. \tag{9}$$

From (6), the derivative of (9) is derived as

$$\begin{aligned}\dot{V}_0 &= \tilde{\boldsymbol{d}}^T(\dot{\boldsymbol{d}} - \frac{M}{\gamma}(\dot{\boldsymbol{x}}_2 + \dot{\boldsymbol{x}}_{2f}) - \dot{\bar{\boldsymbol{\zeta}}}_f)\\ &= \tilde{\boldsymbol{d}}^T(\dot{\boldsymbol{d}} - \frac{1}{\gamma}\tilde{\boldsymbol{d}})\\ &\le -\frac{1}{2\gamma}\tilde{\boldsymbol{d}}^T\tilde{\boldsymbol{d}} + \frac{\gamma}{2}\|\dot{\boldsymbol{d}}\|^2.\end{aligned} \tag{10}$$

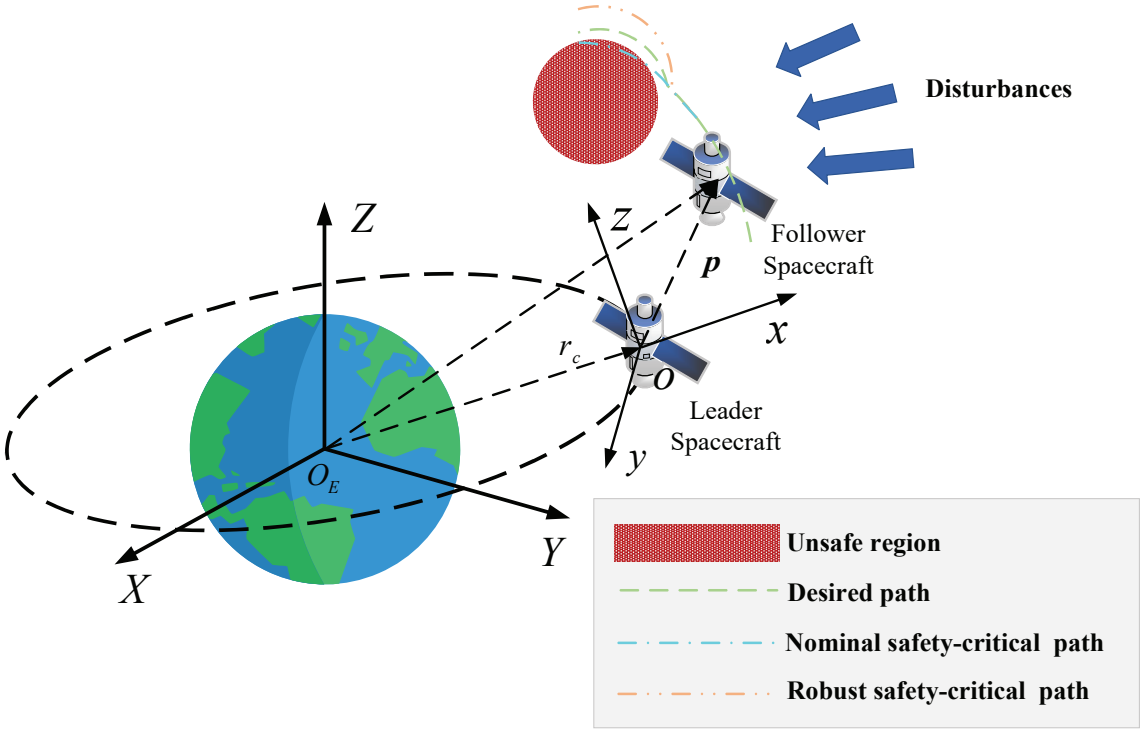

Figure 1. The relative motion of spacecraft with disturbances and obstacles.

From (10), it yields $V_0 \leq \exp(-\frac{t}{\beta})V_0(0) + \frac{\gamma^2 \breve{d}^2}{2}$. *Based on Assumption 1 and the definition of* V_0, *it further yields*

$$\begin{aligned}\|\tilde{\boldsymbol{d}}\| &\leq \left(2\exp(-\frac{t}{\gamma})V_0(0) + \gamma^2\breve{d}^2\right)^{\frac{1}{2}} \\ &\leq \left(\exp(-\frac{t}{\gamma})(\breve{D} + \|\hat{\boldsymbol{d}}(0)\|)^2 + \gamma^2\breve{d}^2\right)^{\frac{1}{2}} \triangleq D(t),\end{aligned} \tag{11}$$

where $D(t)$ *characterizes the convergence region of the estimation error* $\tilde{\boldsymbol{d}}$, *serves as a foundation for deriving the DTCBF conditions in the subsequent control design.*

3.2 FASA Nominal Controller Design

In the case of an ideal orbital environment with $\boldsymbol{u}_{si} = \boldsymbol{0}_{3\times1}, i = 1, \ldots, N$, the tracking error dynamics can be directly obtained from (2) as

$$\dot{\boldsymbol{Z}} = \bar{\boldsymbol{A}}\boldsymbol{Z} + \boldsymbol{g}\Big[(\boldsymbol{u} + \boldsymbol{d} + \boldsymbol{\zeta}) - M\ddot{\boldsymbol{p}}_d\Big], \tag{12}$$

where $\boldsymbol{Z} = [\boldsymbol{z}^T, \dot{\boldsymbol{z}}^T]^T$. $\boldsymbol{z} = \boldsymbol{p} - \boldsymbol{p}_r$ is the tracking error and $\boldsymbol{p}_r$ is the desired relative motion trajectory.

To stabilize the tracking error dynamics (12), the FASA nominal controller is designed as

$$\boldsymbol{u}_0 = -M\Big[\boldsymbol{A}\boldsymbol{Z} - \ddot{\boldsymbol{p}}_d\Big] - \hat{\boldsymbol{d}} - \boldsymbol{\zeta}, \tag{13}$$

where $\boldsymbol{A} = [a_0\boldsymbol{I}_3, a_1\boldsymbol{I}_3] \in \mathbb{R}^{3\times6}$ are a parameter matrix, a_0 and a_1 are the positive constants, $\boldsymbol{I}_3 \in \mathbb{R}^{3\times3}$ is the identity matrix.

Define the Lyapunov function as

$$V = \boldsymbol{Z}^T\boldsymbol{Q}\boldsymbol{Z}, \tag{14}$$

where $\boldsymbol{Q} \in \mathbb{R}^{6\times6}$ is a positive-definite matrix.

From (12), the derivative of (14) is obtained as

$$\dot{V} = \boldsymbol{Z}^T\boldsymbol{Q}\dot{\boldsymbol{Z}} + \dot{\boldsymbol{Z}}^T\boldsymbol{Q}\boldsymbol{Z}. \tag{15}$$

Substituting (13) into (15), one has

$$\begin{aligned}\dot{V} \leq\ & \boldsymbol{Z}^T\Big[\boldsymbol{\Phi}^T\boldsymbol{Q} + \boldsymbol{\Phi}^T\boldsymbol{Q}\Big]\boldsymbol{Z} \\ &+ \Big[\boldsymbol{Z}^T\boldsymbol{Q}\boldsymbol{g}\tilde{\boldsymbol{d}} + \tilde{\boldsymbol{d}}^T\boldsymbol{g}^T\boldsymbol{Q}\boldsymbol{Z}\Big],\end{aligned} \tag{16}$$

where $\boldsymbol{\Phi} = [\mathbf{0}_{3\times3}, \boldsymbol{I}_3; -a_0\boldsymbol{I}_3, -a_1\boldsymbol{I}_3] \in \mathbb{R}^{6\times6}$.

Based on Young's inequality, it can be further yielded as

$$2\boldsymbol{Z}^T\boldsymbol{Q}\boldsymbol{g}\tilde{\boldsymbol{d}} \leq \frac{\lambda_{\max}(\boldsymbol{Q}\boldsymbol{g}(\boldsymbol{Q}\boldsymbol{g})^T)}{\lambda_{\min}(\boldsymbol{Q})}V + \|\tilde{\boldsymbol{d}}\|^2. \tag{17}$$

Invoking (17) into (16), one obtains

$$\dot{V} \leq -kV + D^2, \tag{18}$$

where $k = \delta - \frac{\lambda_{\max}(\boldsymbol{Q}\boldsymbol{g}(\boldsymbol{Q}\boldsymbol{g})^T)}{\lambda_{\min}(\boldsymbol{Q})} > 0$.

Theorem 2 *For the spacecraft system described by (1) and the nominal controller in (13), the relative motion tracking error converges to a small region around the origin*

$$\Omega_z = \Big\{\boldsymbol{Z} \mid V(t) \leq \exp(-kt)V(0) + \frac{D^2}{k}(1-\exp(-kt))\Big\}. \tag{19}$$

Proof 2 *Solve the differential equation (18), it follows that*

$$V(t) \leq \exp(-kt)V(0) + \frac{D^2}{k}(1-\exp(-kt)). \tag{20}$$

It can be concluded that the convergence region of $\boldsymbol{Z}$ is near the origin, which can be denoted as

$$\Omega_z = \Big\{\boldsymbol{Z} \mid V(t) \leq \exp(-kt)V(0) + \frac{D^2}{k}(1-\exp(-kt))\Big\}. \tag{21}$$

3.3 Safety-Critical Controller Design

In this subsection, the control input is defined as $\boldsymbol{u}_i = \boldsymbol{u}_0 + \sum_{i=1}^{N}\boldsymbol{u}_{si}$ where $\boldsymbol{u}_i$ is designed to enforce safety with respect to the unsafe regions O_i. The i-th unsafe region in the spacecraft's orbit is modeled as a spherical set O_i centered at $\boldsymbol{p}_{oi}$ with radius R_{oi}. To encode safety, a barrier function is introduced as: $b_i = \|\boldsymbol{p}-\boldsymbol{p}_{oi}\|^2 - R_{oi}^2$ so that $b_i \geq 0$ ensures the spacecraft remains outside the unsafe sphere. Given that the relative degree of h_i is 2, an auxiliary system is formulated as follows

$$\begin{cases} \varrho_{i,0} = b_i, \\ \varrho_{i,1} = \dot{\varrho}_{i,0} + \eta_{i1}\varrho_{i,0}, \\ \varrho_{i,2} = \dot{\varrho}_{i,1} + \eta_{i2}\varrho_{i,1}, \end{cases} \tag{22}$$

where η_{i1} and η_{i2} are positive constants.

From (22), $\varrho_{i,2}(\boldsymbol{x}, \boldsymbol{u}_i, \boldsymbol{d}, t)$ can be calculated as

$$\begin{aligned} &\varrho_{i,2}(\boldsymbol{x}, \boldsymbol{u}_i, \boldsymbol{d}, t) \\ &\geq 2\|\dot{\boldsymbol{p}} - \dot{\boldsymbol{p}}_{oi}\|^2 + 2(\boldsymbol{p}-\boldsymbol{p}_{oi})^T\Big[\frac{1}{m}(\boldsymbol{u}_i + \boldsymbol{F} + \hat{\boldsymbol{d}}) - \ddot{\boldsymbol{p}}_{oi}\Big] \\ &\quad + 2(\eta_{i1}+\eta_{i2})(\boldsymbol{p}-\boldsymbol{p}_{oi})^T(\dot{\boldsymbol{p}} - \dot{\boldsymbol{p}}_{oi}) + \eta_{i1}\eta_{i2}(\|\boldsymbol{p}-\boldsymbol{p}_{oi}\|^2 \\ &\quad - R_{oi}^2) - 2\frac{\|\boldsymbol{p}-\boldsymbol{p}_{oi}\|}{M}D(t) \\ &= \varrho_{i,2}(\boldsymbol{x}, \boldsymbol{u}_i, \hat{\boldsymbol{d}}, t) - 2\frac{\|\boldsymbol{p}-\boldsymbol{p}_{oi}\|}{M}D(t) \\ &= \varrho_{i,2}(\boldsymbol{x}, \boldsymbol{u}_i, \hat{\boldsymbol{d}}, t) - \|L_{\boldsymbol{g}}L_{\boldsymbol{f}}b_i\|\frac{D(t)}{M}. \end{aligned} \tag{23}$$

Based on the auxiliary system (22), the following set $\mathcal{B}_{i,j}$ is defined as

$$\mathcal{B}_{i,j} = \{(\boldsymbol{x}, \boldsymbol{d}) \in \mathbb{R}^6 \times \mathbb{D} : \varrho_{i,j-1} \geq 0\}, j \in \{1,2\}, \tag{24}$$

where $\mathbb{D}$ is the disturbance set.

Definition 1 *Considering the spacecraft system (1), the disturbance compensation term (7), and the sets (24), a differentiable function $b_i(\boldsymbol{x}) : \mathbb{R}^6 \to \mathbb{R}$ is a DTCBF, if the following condition holds*

$$\sup_{\boldsymbol{u}_i\in\mathbb{R}^3}\Big\{\varrho_{i,2}(\boldsymbol{x}, \boldsymbol{u}_i, \hat{\boldsymbol{d}}, t)\Big\} - \|L_{\boldsymbol{g}}L_{\boldsymbol{f}}b_i\|\frac{D(t)}{M} \geq 0 \tag{25}$$

for all $(\boldsymbol{x}, \boldsymbol{d}) \in \mathcal{B}_{i,1} \cap \mathcal{B}_{i,2}$.

Theorem 3 *Consider a DTCBF associated with the sets $\mathcal{B}_{i,j}, j \in \{1,2\}$ and the disturbance compensation term (7). Provided that the initial states satisfy $(\boldsymbol{x}(0), \boldsymbol{d}(0)) \in \mathcal{B}_{i,1} \cap \mathcal{B}_{i,2}$, the set $\mathcal{B}_{i,1} \cap \mathcal{B}_{i,2}$ is forward invariant for the spacecraft (1) under any continuous control input $\boldsymbol{u}_i(\boldsymbol{x}, \hat{\boldsymbol{d}}) \in \mathcal{U}_i$ belonging to the admissible set $\mathcal{U}_i \triangleq \{\boldsymbol{u}_i \in \mathbb{R}^3 : \varrho_{i,2}(\boldsymbol{x}, \boldsymbol{u}_i, \hat{\boldsymbol{d}}, t) - \|L_{\boldsymbol{g}}L_{\boldsymbol{f}}b_i\|\frac{D(t)}{M} \geq 0\}$.*

Proof 3 *Given that $\boldsymbol{u}_i(\boldsymbol{x}, \hat{\boldsymbol{d}}) \in \mathcal{U}_i$, it follows that $\varrho_{i,2}(\boldsymbol{x}, \boldsymbol{u}_i, \boldsymbol{d}, t) \geq \varrho_{i,2}(\boldsymbol{x}, \boldsymbol{u}_i, \hat{\boldsymbol{d}}, t) - \|L_{\boldsymbol{g}}L_{\boldsymbol{f}}b_i\|\frac{D(t)}{m} \geq 0$, and furthermore, $\dot{\varrho}_{i,1} + \eta_{i2}\varrho_{i,1} \geq 0$. With the initial condition $(\boldsymbol{x}(0), \boldsymbol{d}(0)) \in \mathcal{B}_2$, Lemma 2 ensures that $\varrho_{i,1}(\boldsymbol{x}, t) \geq 0, \forall t > 0$, which establishes the forward invariance of $\mathcal{B}_{i,2}$. Similarly, from (22) and the initial condition $(\boldsymbol{x}(0), \boldsymbol{d}(0)) \in \mathcal{B}_{i,1}$, the Lemma 2 yields $\varrho_{i,0}(\boldsymbol{x}, t) \geq 0, \forall t > 0$, guaranteeing that the set $\mathcal{B}_{i,1}$ is forward invariant. Consequently, the intersection set $\mathcal{B}_{i,1} \cap \mathcal{B}_{i,2}$ remains forward invariant.*

To simultaneously ensure the stability and safety of the spacecraft relative motion tracking system, a QP problem that integrates the nominal controller $\boldsymbol{u}_{i-1}$

with the DTCBF constraints as follows

$$\begin{cases} \boldsymbol{u}_i^* = \arg\min\limits_{\boldsymbol{u}_{si}\in\mathbb{R}^3} \|\boldsymbol{u}_i - \boldsymbol{u}_{i-1}\|^2, \\ \text{s.t.} \quad -\varpi_i - L_{\bar{\boldsymbol{L}}} L_{\boldsymbol{f}} h_i \dfrac{1}{m}\boldsymbol{u}_{si} \le 0, \end{cases} \tag{26}$$

where

$$\varpi_i = \varrho_{i,2}(\boldsymbol{x}, \boldsymbol{u}_{i-1}, \hat{\boldsymbol{d}}, t) - \|L_{\boldsymbol{g}} L_{\boldsymbol{f}} b_i\| \frac{D(t)}{M}. \tag{27}$$

Theorem 4 *Under the DTCBF constraints (25) on the nominal input $\boldsymbol{u}_{i-1}$ and the assumption that $L_{\boldsymbol{g}} L_{\boldsymbol{f}} b_i \neq \boldsymbol{0}_{1\times 3}$ for all $(\boldsymbol{x}, \boldsymbol{d}) \in \mathcal{B}_{i,1} \cap \mathcal{B}_{i,2}$, the solution to the QP problem (26) is given by*

$$\boldsymbol{u}_{si} = \begin{cases} \boldsymbol{0}_{3\times 1}, & \varpi_i \ge 0, \\ -M\varpi_i \Big((L_{\boldsymbol{g}} L_{\boldsymbol{f}} b_i)^T \Big)^+, & \varpi_i < 0, \end{cases} \tag{28}$$

where $(\bullet)^+$ is denoted as the Moore-Penrose pseudoinverse.

Proof 4 *Define the Lagrangian function as*

$$\mathcal{L}_i = \|\boldsymbol{u}_{si}\|^2 - \lambda_{i,\mathcal{L}} (\varpi_i + L_{\boldsymbol{g}} L_{\boldsymbol{f}} b_i \frac{1}{M} \boldsymbol{u}_{si}), \tag{29}$$

where $\lambda_{i,\mathcal{L}}$ is a positive constant.

From (29), the Karush-Kuhn-Tucker conditions can be obtained as follows

$$\begin{cases} \dfrac{\partial \mathcal{L}_i}{\partial \boldsymbol{u}_{si}} = 2\boldsymbol{u}_{si} - \dfrac{\lambda_{i,\mathcal{L}}}{m} (L_{\boldsymbol{g}} L_{\boldsymbol{f}} b_i)^T = \boldsymbol{0}_{3\times 1}, \\ \lambda_{i,\mathcal{L}} (\varpi_i + L_{\boldsymbol{g}} L_{\boldsymbol{f}} b_i \dfrac{1}{M} \boldsymbol{u}_{si}) = 0, \\ \lambda_{i,\mathcal{L}} \ge 0. \end{cases} \tag{30}$$

Case 1: The condition $\lambda_{i,\mathcal{L}} = 0$ yields $\boldsymbol{u}_{si} = \boldsymbol{0}_{3\times 1}$ with $\eta \ge 0$, implying the safety constraint is not triggered. Consequently, the spacecraft remains safe under the sole action of the nominal controller $\boldsymbol{u}_{i-1}$, and no additional safety correction is needed.

Case 2: The condition $\lambda_{i,\mathcal{L}} > 0$ leads to a non-zero safety correction $\boldsymbol{u}_{si} = -M\varpi_i((L_{\boldsymbol{g}} L_{\boldsymbol{f}} b_i)^T)^+$, which activates the safety constraint. Here, system safety is enforced solely by the corrective action $\boldsymbol{u}_{si}$.

Remark 1 *Unlike the methods reported in [17–23], the proposed approach sequentially processes each unsafe region's CBF constraints by introducing a safety correction term $\boldsymbol{u}_{si}$, thereby synthesizing a composite control input that ensures safety across all forbidden zones. The detailed implementation procedure is outlined in Algorithm 1.*

Algorithm 1: Sequential Correction-Based Strategy

Input: The nominal controller $\boldsymbol{u}_0$ in (13) and the unsafe region set $O(1, \ldots, N)$.
Output: The safety-critical controller $\boldsymbol{u} = \boldsymbol{u}_N$.
initialization: Set $\boldsymbol{u}_n = \boldsymbol{u}_0$, and assume $\bigcap_{i=1}^N \mathcal{U}_i \neq \varnothing$;
while $i = 1, \ldots, N$ **do**
  Define the DTCBF constraint (25) corresponding to the ith unsafe region;
  Determine the safety correction term $\boldsymbol{u}_{i-1}$ via the QP formulation (26), with $\boldsymbol{u}_{si}$ as the nominal input;
  Update the controller to $\boldsymbol{u}_i = \boldsymbol{u}_{i-1} + \boldsymbol{u}_{si}$ using the solution from (28);
end

4 Simulations

Numerical simulations are conducted to validate the effectiveness of the proposed control scheme for spacecraft relative motion with obstacle avoidance. The relevant system parameters are set as $e_c = 0.02$, $a_c = 7000$km, and $M = 20$kg. The initial states of the spacecraft system and the low-pass filters are set as $\boldsymbol{p}(0) = [20, -20, 10]^T$, $\dot{\boldsymbol{p}}(0) = [0, 0, 0]^T$, $\boldsymbol{x}_{2f}(0) = [0, 0, 0]^T$, and $\bar{\boldsymbol{F}}_f(0) = [0, 0, 0]^T$. The reference relative motion trajectory and external disturbance are set as $[-20\sin(0.02t), 0.5t, -20\cos(0.02t)]^T$m and $\boldsymbol{d} = 0.5[\cos(0.05t), -\sin(0.05t), -\cos(0.05t)]^T$N. The control parameters are set as $a_0 = 0.01$, $a_1 = 0.2$, $\delta = 0.05$, and $\eta_{i1} = \eta_{i2} = 0.5$. Two spherical obstacles of radius 7m are introduced: one is stationary at $\boldsymbol{p}_{o1} = [-7.35, 7.32, -3.76]^T$, and the other is dynamic with its trajectory governed by $\boldsymbol{p}_{o2} = [-30.83 + 0.2t, 88 - 0.05t, 24.53 - 0.02t]^T$.

The simulation results are presented in Figures 2–8. Figure 2 depicts the spacecraft trajectory, with dark red spheres denoting obstacles. Figures 3 and 4 illustrate the relative position p and tracking error z, respectively, demonstrating the spacecraft's ability to track the target while avoiding obstacles. The control input in Figure 5 exhibits a noticeable increase when the spacecraft approaches obstacles, reflecting the active safety correction. Figure 6 shows the estimation error of the unknown dynamic estimator, confirming its effectiveness in approximating external disturbances.

The obstacle avoidance performance under different control barrier functions is compared in Figures 7 and 8. Specifically, the standard CBF does not account for system disturbances, leading to safety

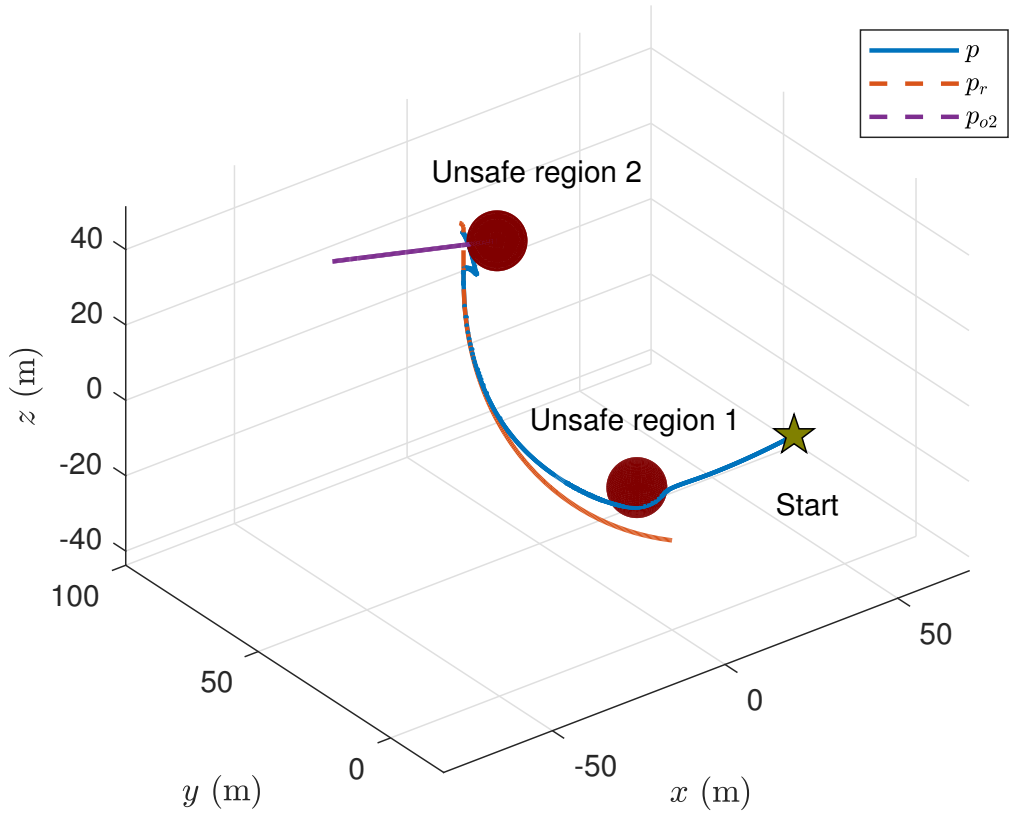

Figure 2. The motion trajectory of follower spacecraft.

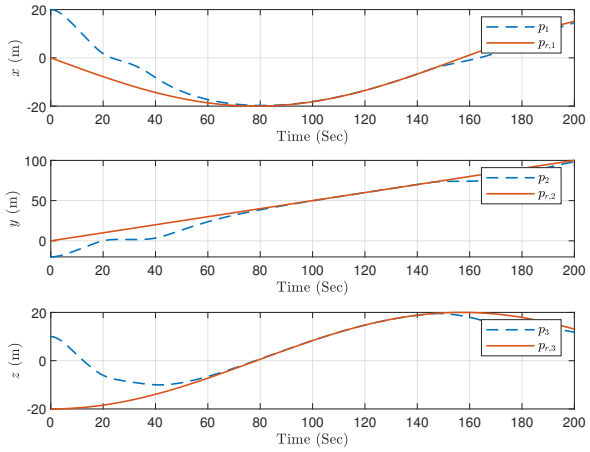

Figure 3. The relative motion tracking performance.

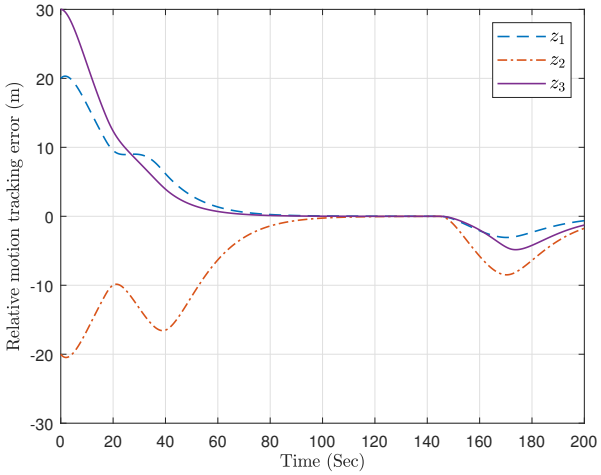

Figure 4. The tracking error z.

constraint violations under external disturbances. The robust CBF, designed based on worst-case disturbances, ensures safety but results in overly conservative trajectories. In contrast, the proposed disturbance rejection CBF strictly enforces obstacle avoidance constraints without excessive conservatism, demonstrating its superior robustness and practicality.

5 Conclusion

This paper has developed a safety-critical control scheme within the FASA framework to address the dual challenges of precise relative motion tracking and safety assurance for spacecraft operating under external disturbances and multiple forbidden regions.

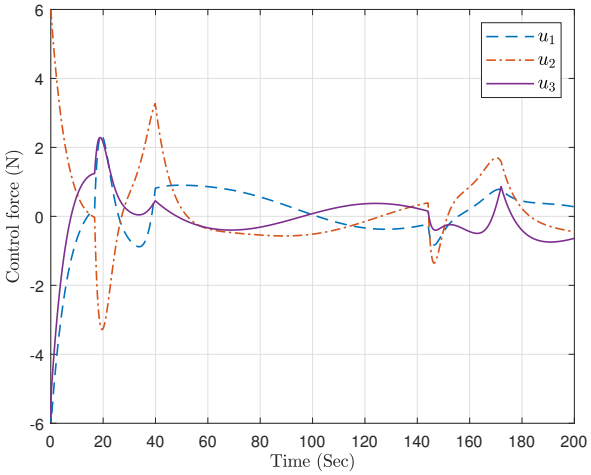

Figure 5. The control force $\boldsymbol{u}$.

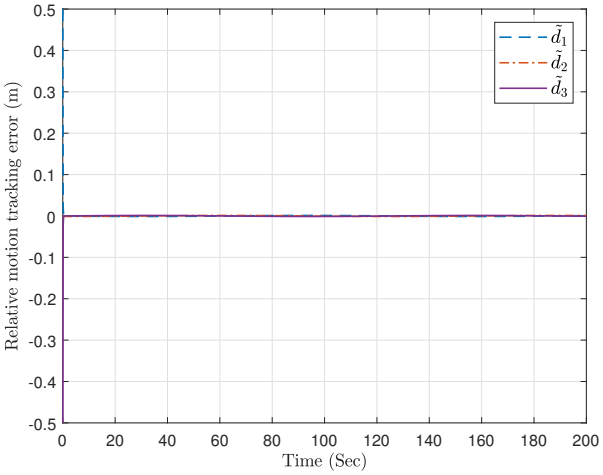

Figure 6. The estimation error $\tilde{\boldsymbol{d}}$.

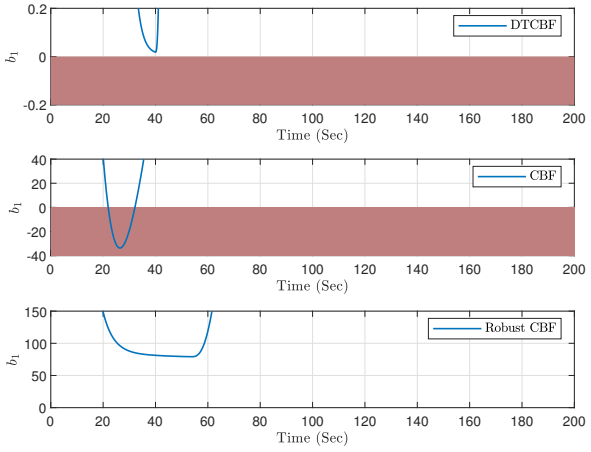

Figure 7. The barrier function b_1 under DTCBF, conventional CBF, and robust CBF conditions.

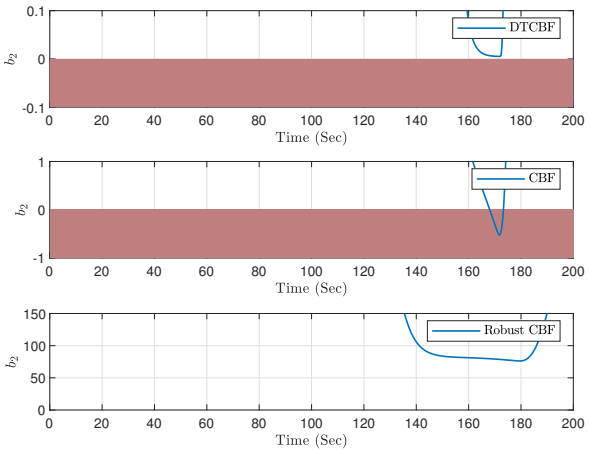

Figure 8. The barrier function b_2 under DTCBF, conventional CBF, and robust CBF conditions.

The proposed methodology demonstrates that through FASA-based nominal controller design, tracking performance can be achieved with simplified control synthesis while maintaining theoretical guarantees. For safety constraints, the introduced DTCBF with integrated disturbance compensation effectively mitigates interference effects, and the novel sequential correction strategy enables constraint enforcement through offline-computed solutions, thereby eliminating dependency on real-time optimization. Theoretical guarantees establish the framework's capability to ensure both collision avoidance and tracking performance.

Data Availability Statement

Data will be made available on request.

Funding

This work was supported in part by the National Natural Science Foundation of China under Grant U25A20452, Grant 62222315, Grant 61973274, Grant 62233016, and Grant 62203384; in part by the Zhejiang Provincial Natural Science Foundation of China under Grant LZ26F030004; in part by the Fundamental Research Funds for the Provincial Universities of Zhejiang under Grant RF-C2024001.

Conflicts of Interest

The authors declare no conflicts of interest.

AI Use Statement

The authors declare that no generative AI was used in the preparation of this manuscript.

Ethical Approval and Consent to Participate

Not applicable.

References

[1] Shi, Y., Hu, Q., Li, D., & Lv, M. (2023). Adaptive optimal tracking control for spacecraft formation flying with event-triggered input. *IEEE Transactions on Industrial Informatics, 19*(5), 6418–6428. [CrossRef]

[2] Guelman, M., Kogan, A., Kazarian, A., Livne, A., Orenstein, M., & Michalik, H. (2005). Acquisition and pointing control for inter-satellite laser communications. *IEEE Transactions on Aerospace and Electronic Systems, 40*(4), 1239-1248. [CrossRef]

[3] Cui, B., Xia, Y., Liu, K., Wang, Y., & Zhai, D. H. (2019). Velocity-observer-based distributed finite-time attitude tracking control for multiple uncertain rigid spacecraft. *IEEE Transactions on Industrial Informatics, 16*(4), 2509-2519. [CrossRef]

[4] Horstkötter, E., & Zhu, Q. (2025). Computational experimental test on PID controlled fixed wing aircraft systems. *ICCK Transactions on Sensing, Communication, and Control, 2*(2), 95–105. [CrossRef]

[5] Xiang, K., Song, Y., & Ioannou, P. (2025). Nonlinear adaptive PID control for nonlinear systems. *IEEE Transactions on Automatic Control, 70*(10), 7000–7007. [CrossRef]

[6] Gao, S., Hou, Y., Dong, Y., & Li, S. (2020). Global nested PID control of strict-feedback nonlinear systems with prescribed output and virtual tracking performance. *IEEE Transactions on Circuits and Systems II: Express Briefs, 67*(2), 325–329. [CrossRef]

[7] Wang, S., & Wang, X. (2025). Fixed-time adaptive optimal parameter estimation subject to dead-zone and control of servo systems. *ICCK Transactions on Sensing, Communication, and Control, 2*(3), 200–214. [CrossRef]

[8] Wang, S., Sun, C., Chen, Q., & He, H. (2025). Composite learning fixed-time control for nonlinear servo systems with state constraints and unknown dynamics. *IEEE Transactions on Systems, Man, and Cybernetics: Systems, 55*(3), 2332–2342. [CrossRef]

[9] Lei, Y., Wang, Z., Wang, X., Li, H., & Morărescu, I. C. (2025). Hybrid formation control for heterogeneous uncertain linear two-time-scale systems. *Automatica, 176*, 112267. [CrossRef]

[10] Shi, H., Xie, S., Chen, Q., Hu, S., & Yi, S. (2024). Adaptive tunable predefined-time backstepping control for uncertain robotic manipulators. *ICCK Transactions on Sensing, Communication, and Control, 1*(2), 126–135. [CrossRef]

[11] Yang, X., Chen, Q., Xie, S., & He, X. (2025). Adaptive predefined-time event-triggered control for attitude consensus of multiple spacecraft with time-varying state constraints. *IEEE Transactions on Systems, Man, and Cybernetics: Systems, 55*(6), 3756–3768. [CrossRef]

[12] An, J., Cao, L., Wang, Y., Jadoon, A. K., & Wang, S. (2024). Adaptive Fault-Tolerant Optimized Platoon Cloud Tracking Control for Heterogeneous Vehicles via Dual Learning Mechanism. *IEEE Transactions on Automation Science and Engineering, 22*, 4382-4393. [CrossRef]

[13] Duan, G. R. (2020). High-order system approaches: I. Fully-actuated systems and parametric designs. *Acta Automatica Sinica, 46*(7), 1333–1345. [CrossRef]

[14] Zhang, D., Liu, G., & Cao, L. (2023). Proportional integral predictive control of high-order fully actuated networked multiagent systems with communication delays. *IEEE Transactions on Systems, Man, and Cybernetics: Systems, 53*(2), 801–812. [CrossRef]

[15] Zhao, Q., & Duan, G. R. (2022). Fully actuated system approach for 6DOF spacecraft control based on extended state observer. *Journal of Systems Science and Complexity, 35*(2), 604–622. [CrossRef]

[16] Duan, G., & Liu, G. P. (2022). Attitude and orbit optimal control of combined spacecraft via a fully-actuated system approach. *Journal of Systems Science and Complexity, 35*(2), 623–640. [CrossRef]

[17] Cortez, W. S., Oetomo, D., Manzie, C., & Choong, P. (2021). Control barrier functions for mechanical systems: Theory and application to robotic grasping. *IEEE Transactions on Control Systems Technology, 29*(2), 530–545. [CrossRef]

[18] Zhang, S., Zhai, D. H., Lin, J., Xiong, Y., Xia, Y., & Wei, M. (2024). ESO-based safety-critical control for robotic systems with unmeasured velocity and input delay. *IEEE Transactions on Industrial Electronics, 71*(10), 13053–13063. [CrossRef]

[19] Xu, X. (2018). Constrained control of input–output linearizable systems using control sharing barrier functions. *Automatica, 87*, 195–201. [CrossRef]

[20] Ames, A. D., Xu, X., Grizzle, J. W., & Tabuada, P. (2016). Control barrier function based quadratic programs for safety critical systems. *IEEE Transactions on Automatic Control, 62*(8), 3861–3876. [CrossRef]

[21] Xiao, W., & Belta, C. (2021). High-order control barrier functions. *IEEE Transactions on Automatic Control, 67*(7), 3655–3662. [CrossRef]

[22] Nguyen, Q., & Sreenath, K. (2021). Robust safety-critical control for dynamic robotics. *IEEE Transactions on Automatic Control, 67*(3), 1073–1088. [CrossRef]

[23] Wang, X., Yang, J., Liu, C., Yan, Y., & Li, S. (2024). Safety-critical disturbance rejection control of nonlinear systems with unmatched disturbances. *IEEE Transactions on Automatic Control, 70*(4), 2722–2729. [CrossRef]

[24] Liu, J., Sun, M., Chen, Z., & Sun, Q. (2019). Output feedback control for aircraft at high angle of

attack based upon fixed-time extended state observer. *Aerospace Science and Technology, 95*, 105468. [CrossRef]

[25] Duan, G. (2021). High-order fully actuated system approaches: Part V. Robust adaptive control. *International Journal of Systems Science, 52*(10), 2129–2143. [CrossRef]

[26] Glotfelter, P., Cortés, J., & Egerstedt, M. (2017). Nonsmooth barrier functions with applications to multi-robot systems. *IEEE Control Systems Letters, 1*(2), 310–315. [CrossRef]

[27] Na, J., Jing, B., Huang, Y., Gao, G., & Zhang, C. (2020). Unknown system dynamics estimator for motion control of nonlinear robotic systems. *IEEE Transactions on Industrial Electronics, 67*(5), 3850–3859. [CrossRef]

Xiaoyu Yang received the B.E degree in automation from Northeast University at Qinhuangdao, Qinhuangdao, China, in 2019, and the M.S. degree in control science and engineering from Bohai University, Jinzhou, China, in 2023. He is currently working toward the Ph.D. degree in control science and engineering with the Zhejiang University of Technology, Hangzhou, China.

His research interests include safety-critical control and finite-time control with application to spacecraft system. (Email: yangxiaoyubhu@163.com)

Qiang Chen received the B.S. degree in measure and control technology and instrumentation from Hebei Agricultural University, Baoding, China, in 2006 and the Ph.D. degree in the control science and engineering from Beijing Institute of Technology, Beijing, China, in 2012.

Since 2012, he has been with the College of Information Engineering, Zhejiang University of Technology, Hangzhou, China, where he was a Professor, in 2022. He has published over 100 peer-reviewed papers in journals and conference proceedings, and has been authorized more than 60 invention patents, 13 of which were transferred. His research interests include adaptive control and iterative learning control with application to motion control systems. (Email: sdnjchq@zjut.edu.cn)

Xiongxiong He received the M.S. degree in operation and control from Qufu Normal University, Qufu, China, in 1994, and the Ph.D. degree in control science and engineering from Zhejiang University, Hangzhou, China, in 1997.

He held a post-doctoral position with the Harbin Institute of Technology from 1998 to 2000. He joined the Zhejiang University of Technology Hangzhou, China, in 2001, where he has been a Professor with the College of Information Engineering. (Email: hxx@zjut.edu.cn)